Accepted Manuscript

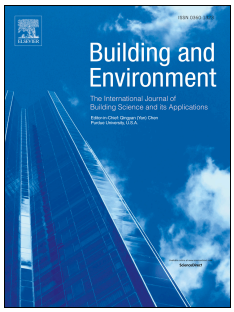

Parametric study of air curtain door aerodynamics performance based on experiments and numerical simulations

Dahai Qi, Sherif Goubran, Liangzhu (Leon) Wang, Radu Zmeureanu

PII: S0360-1323(17)30563-2

DOI: 10.1016/j.buildenv.2017.12.005

Reference: BAE 5203

To appear in: *Building and Environment*

Received Date: 21 September 2017

Revised Date: 4 December 2017

Accepted Date: 8 December 2017

Please cite this article as: Qi D, Goubran S, Wang L(L), Zmeureanu R, Parametric study of air curtain door aerodynamics performance based on experiments and numerical simulations, *Building and Environment* (2018), doi: 10.1016/j.buildenv.2017.12.005.

Parametric Study of Air Curtain Door Aerodynamics Performance Based on Experiments and Numerical Simulations

Dahai Qi, Sherif Goubran, Liangzhu (Leon) Wang, Radu Zmeureanu

Centre for Zero Energy Building Studies, Department of Building, Civil and Environmental Engineering, Concordia University, 1455 de Maisonneuve Blvd. West, Montreal, Quebec, H3G 1M8, Canada

Abstract

Air curtains have been widely used to reduce infiltration through door openings and save heating/cooling energy in different types of buildings. Previous studies have found that there exist three aerodynamics conditions: optimum condition (OC), inflow break-through (IB), and outflow break-through (OB) conditions, which are important for categorizing air curtain performance subject to such key parameters including supply speed and angle, and presence of a person during an actual operation. However, few studies have focused on the effects of these parameters on air curtain performance in terms of resisting infiltration and reducing exfiltration. This research presents a parametric study of air curtain performance based on reduced-scale experiments and full-scale numerical simulations. It was found that increasing air curtain supply angle improves air curtain performance when it is operated under the OC and IB conditions but creates excessive exfiltration under the OB condition. Increasing supply speed of air curtain generally improves the air curtain performance whereas this improvement deteriorates with the increase of supply angle under the OB condition. The presence of person, either directly under or below the air curtain, almost has no effect on the infiltration/exfiltration during the OC condition. Moreover, the person in the doorway can block airflow from both directions, contributing to less infiltration under the IB condition and less exfiltration under the OB condition than without the person. This study provides valuable insights into air curtain aerodynamics performance under different operational conditions and key contributing parameters.

Keywords: air curtain; buildings; aerodynamics; experiments; CFD; parametric study

1. Introduction

Every year, buildings use large amounts of energy. It is reported that, in the U.S., the building sector, including residential, commercial and government buildings, accounted for about 41% of the primary energy usage, 47% of which is used for the space heating and cooling systems [1]. For the commercial buildings, air infiltrations can contribute to 18% of the total heat loss [2]. In modern well-constructed and well insulated buildings, heat losses due to air infiltration become more significant and is estimated to be responsible for up to 25% of the building heating loads [3]. Infiltrations through door openings become quite significant when the doors are frequently used such as in restaurants, retail stores, supermarkets, offices, and hospitals [4].

A common solution to reduce energy loss due to air infiltration through door opening is to use a vestibule instead of single doors [5,6]. Yuill [7] and Yuill et al. [8] conducted one of the pioneer studies to estimate infiltration rates for automatic doors based on door usage frequency, geometry, and the pressure difference across a door. It was found that a building entrance with a vestibule has a smaller discharge coefficient, C_D, and therefore it results in the reduction of air infiltrations when compared to the entrances without a vestibule (i.e. single doors) [7]. For this reason, vestibules became a requirement in climate zones 3 ~ 8 based on the ASHRAE Standard 90.1 [9]. Air curtains have been proposed and supported by previous studies [10,11] as an alternative way to decreasing the infiltration rates through the building entrance and reducing building energy heat losses. The air curtains, which are typically mounted above doorways, separate indoor and outdoor temperatures with a stream of air strategically engineered to strike the floor with a particular velocity and position [12]. Since the infiltration rate through building entrance is directly related to the energy performance of air curtains, many studies focused on the air jet aerodynamics and its relationship with the infiltration rate [13–18]. Hayes [19] and Hayes and Stoecker [20] proposed an analytical model in terms of “deflection modulus”, a ratio of air curtain jet momentum to transverse forces, as a result of temperature difference through air curtain. Based on the analytical model, the minimum jet outlet momentum to ensure air jet reaching the floor could be determined, which was defined as the “optimum condition” pattern in their research. If the minimum jet outlet momentum was not satisfied, the air curtain jet would not reach the floor, which is called “break-through condition”. There also existed numerical studies [12,18] on the influence of the

dynamic and geometrical parameters on air curtain performance. Foster et al. [14] simulated a 1.0 m wide air curtain by a 2-D CFD model and noticed that the air curtain performance is directly influenced by jet velocity and door opening duration. By analyzing the CFD simulation results, Wang and Zhong [21] found and defined three airflow patterns: the optimum condition (OC), inflow (or infiltration) break-through (IB) condition, and outflow (or exfiltration) break-through (OB) condition. The infiltration models for door opening with air curtain were also proposed in terms of the pressure difference, flow coefficients, and modifiers, and could be correlated using CFD simulation data for each flow pattern. An experimental study was conducted by Goubran et al. [22] to validate the infiltration models. Using the infiltration models, energy and airflow simulations were employed to calculate the energy consumption in buildings with vestibules and air curtains [4,11]. It was found that, on national level based on the US climate zones, air curtains are more efficient than vestibules in terms of whole building site end-use energy savings and thus outperforming the efficiency of vestibule [11]. However, these studies focused on a specific air curtain supply velocity and angle: for example, the air supply speed and angle were only 15 m/s and 20° in Wang and Zhong's study [21], and 9.1 m/s and 13.75 m/s and 20° in Goubran et al.'s study [22]. The effect of key parameters, e.g., air supply speed and angles on infiltration rate at different flow patterns is unavailable [22]. These are the key parameters for air curtain designs and applications. Moreover, the influence of the people passing through an air curtain door on air curtain performance has not been well addressed.

This research aims to study the effect of supply speed, angle and people on air curtain performance in terms of reducing infiltration and/or exfiltration through a building entrance doorway. Both reduced-scaled experiments and full-size numerical simulation were conducted. This paper first introduced the infiltration models for different air curtain flow patterns from our previous work [21]. Using a similar experimental setup as Goubran et al. [22], we then conducted experimental and numerical analysis of the effects of air curtain supply speed, angle and presence of people in doorway on air curtain performance under different flow patterns and conditions.

2. Methodology

To investigate the effect of air supply speed, angle and people standing under/below the air curtain on the performance of air curtains at building entrances, both reduced-scaled experiments and full-size numerical simulation were employed, which is illustrated in the following sub-sections. The infiltration

model of the door with air curtain is also presented in this section, which is used to evaluate the air curtain performance.

2.1. Experiments

The experiments were conducted in the CUBE (Concordia University Building Environment) chamber (Fig. 1), which comprises an airtight chamber with a blaster door fan, an entrance door installed with an air curtain, pressure sensors located inside of the enclosure, and a laser PIV system to capture airflow patterns through the entrance door [23]. The CUBE is divided into two sections by a horizontal ceiling, and the experiments were conducted in the lower section of 2.44 m × 2.44 m × 1.3 m (L × W × H) [22]. the door size is 0. 61 m × 71 m (W × H). In this study, the door is fully opened. The air curtain supply slot is 0.0635 m × 0.61 m (D × W) with three discharge vanes, which could be adjusted to change the supply angle. The air curtain unit also includes a variable frequency drive (VFD) controller to control the supply speed. The supply speed was measured at 45 points across the supply slot, from which the average speed was obtained. In this study, two different supply velocities were selected: (1) the maximum supply speed of the unit is 13.75 m/s; and (2) a lower speed 9.1 m/s.

The blower door fan is used to control a given pressure difference, ΔP, across the door by depressurization or pressurization. Based on the conservation of mass, the mass air flow rate through the door is equal to the airflow rate through the fan. The duct ending inside the chamber was equipped with an air diffuser to avoid direct flow towards the door (see Fig. 1b). The interior pressures of the chamber were measured and averaged over four points at the chamber's mid-depth plane (Fig. 1a). The external pressure was measured at a point far from the chamber to avoid any possible potential airflow disturbance. The pressure difference across the door was calculated based on the difference between the pressures inside and outside the chamber.

Based on the equipment and setup used, the flow rate achieved from the blower door fan was with a maximum of approximately 0.4 m^3/s infiltration into the chamber and a minimum of approximately 0.3 m^3/s exfiltration from the chamber with the entrance doors fully open. The temperature of the laboratory where the CUBE is located was recorded during the testing and averaged at 23 °C, which was used to calculate the density of the ambient air.

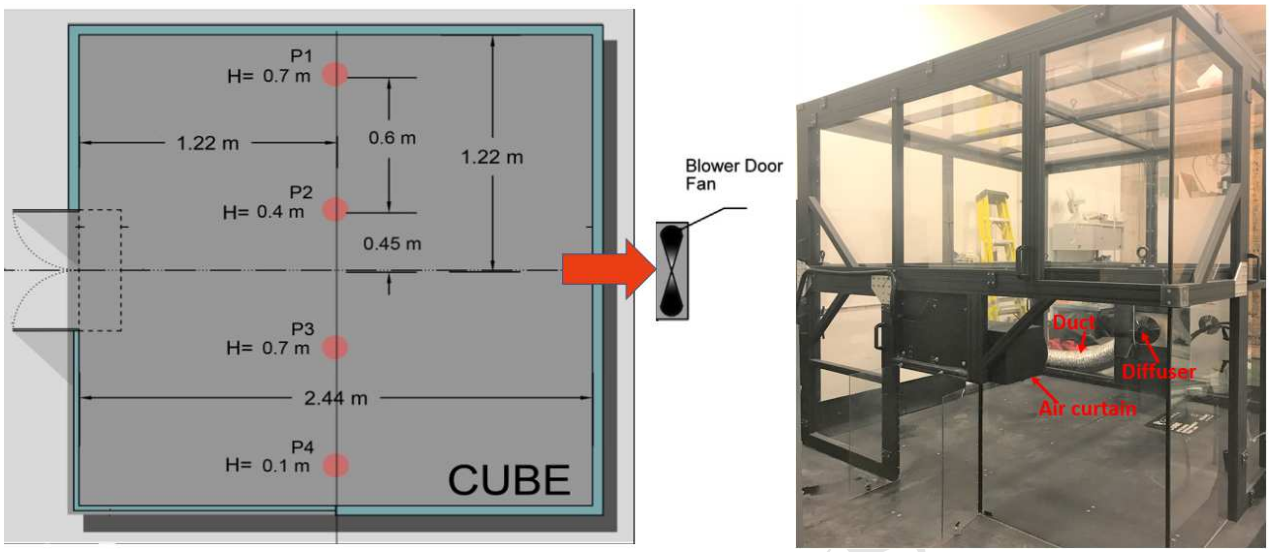

(a) (b)

Fig. 1. The CUBE experimental chamber – (a) top view with locations of the pressure reading points/nodes, and (b) 3D view.

To study the effect of people in the door way on the air curtain performance, a person model was created and placed in the doorway of the air curtain door. Experimental measurements were taken with this setup. The person model and its location about the doorway and the setup are illustrated in Fig. 2. A particle image velocimetry (PIV) system was used for this study to visualize the airflow fields at the doorway with and without a person, which includes a Ng:YAG dual laser head system, the CCD camera [23,24], a specially designed Helium Filled Soap Bubbles (HFSB) system [22], and the PIV data acquisition. Details of the PIV system could be referred to the literature [22] and references on the use of HFSB seeds in large scale measurements can also be found in literature [25,26]. The procedure of processing for the PIV captured velocity data was (1) to correlate the data using the adaptive correlation method with an overlap of 50% (central differencing method with 1.2/2 min peak for validation and an acceptance factor of 0.1), (2) to filter the correlated data using the average filter (3×3 averaging area), and (3) to generate the RMS values of the velocity vectors. The flow scale was generated by using the velocity ranges observed in the cases, and the average error calculations were based on the standard deviation data reported by the software. It is noted that the PIV experiment system may incur errors and uncertainties, due to the systemic errors and the random sampling deviation of statistical errors [27]. Previous studies indicate that though the estimations of PIV measurement accuracy are case by case, it is reasonable to estimate the overall accuracy as approximately 10% at most [27,28].

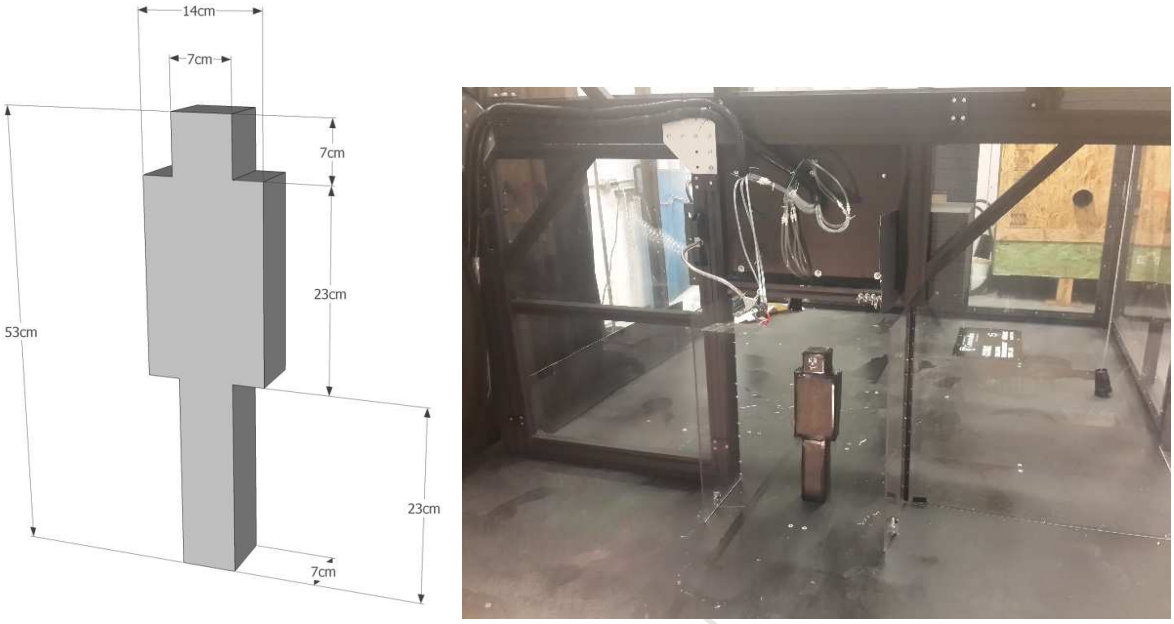

Fig. 2. Details of the person model used and the model placed in the doorway

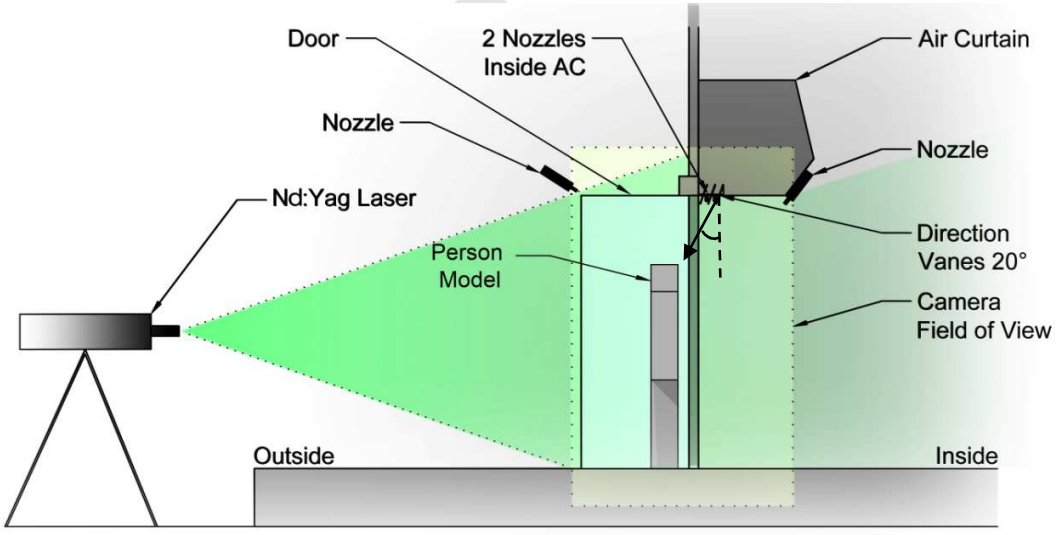

Fig. 3 Illustration of the section view with the field of view and seeding (nozzle) positions highlighted (bottom) (adapted from [11]).

In order to study the effect of air supply speed, angle and presence of people on the air curtain performance, five scenarios, comprised 51 conditions, were selected to be measured in the CUBE (Table 1). The supply angles are 0° and 20° (towards the outside of the door, Fig. 3). The supply air speed is 9.1 m/s and 13.75 m/s. Each condition was repeated twice to ensure the repeatability of the tests.

Table 1. Experimental scenarios.

Scenario	Supply angle (°)	Supply speed (m/s)	With/without people	Measurements	PIV measurements
Scenario 1	0	9.1	without people	7	/
Scenario 2	20	9.1	without people	15	12 (incl. 3 repeated)
Scenario 3	0	13.75	without people	8	/
Scenario 4	20	13.75	without people	16	12 (incl. 3 repeated)
Scenario 5	20	13.75	with people	5	2

2.2. Full-size CFD simulations

The experimental study was conducted for a limited number of conditions under a reduced-scale setup, e.g. only supply angles at 0° and 20° were selected. As a complementary approach, a series of CFD simulations were conducted using the ANSYS FLUENT software, which is widely used to simulate airflows in and/or around buildings [29,30]. The simulations were on a full-size building with the door size of 2 m × 2.4 m (W × H), which is chosen according to the Automatic Door Selection Guide [31]. The full-size CFD simulation model is 3.3:1 of the scaled CUBE chamber. Please note that in the current study, we did not try to compare the results at different scales quantitatively and to develop similarity rules. So the results of the scaled CUBE chamber and the full-size simulation model were only compared qualitatively. Currently, we are developing a new scaling method of air curtain jet flows, which will be covered in a future study. The modeled building section is 20 m × 24 m × 10 m (L × W× H), within a CFD domain of 50 m × 24 m × 10 m (L × W× H). An air curtain is mounted horizontally over the door with a supply slot of 0.08 m × 2 m (W × L) and a return of 0.2 m × 2 m (W × L). When the person is considered in the simulation, the height of the person model is the average height of the Canadian, 1.76 m [32]. Two different locations of people are considered: people directly under the air curtain and below the air curtain (Fig. 4).

To reflect the reality, non-isothermal conditions were considered. The air supply temperature is maintained the same as the indoor temperature: 24 ˚C for the summer condition and 21 ˚C for the winter condition. The air supply angle is varied between 0˚ to 20˚ towards outdoors. Pressure boundaries are applied to the inlet and outlet in Fig. 4, between which the pressure difference varies from -20 Pa to 40 Pa accounting for exterior wind effect. Based on the design day temperatures of the climate zones 1 to 8 in the U.S. [9], the outdoor temperature is selected as -40˚C, -20˚C and 10˚C for the winter mode and 25˚C, 30˚C and 40˚C for the summer mode. In all the simulation cases, the door is fully open (i.e. double swing automatic door with both leaves open at 90°).

The standard k-ε turbulence model was selected as the turbulence model, and the pressure-velocity coupling adopted the SIMPLE algorithm [33]. Standard wall functions and full buoyancy effect were selected. The air was assumed as incompressible ideal gas. Convergence was reached when the residual was less than 10^{-3}, except temperature, which was less than 10^{-6}. The air curtain boundary condition is set up as an inlet with velocity and angle. The fixed mass flow rate was set for the air curtain return, which equals to that of the air curtain supply. The turbulent intensity and hydraulic diameter are used to specify the turbulence, where the turbulent intensity is $I = 0.16\left(\mathrm{Re}_{D_H}\right)^{-1/8}$ [34]. For the spatial discretization scheme, the second order was chosen for the pressure interpolation, and the second order upwind for momentum and energy interpolations. The first order accuracy was chosen for other interpolations. All the grids were structured hexahedral grids. Two different meshing strategies were adopted for the grid independent study. Strategy 1: the grid size of the inlet of air curtain was 0.02 m × 0.02 m. Far-field domain used a coarser grid with the size of 0.2 m × 0.2 m. The total number of the grids was about 1,260,000. Strategy 2: the grid size of the inlet of air curtain was 0.01 m × 0.01 m. Far-field domain used a coarser grid with the size of 0.15 m × 0.15 m. The total number of the grids was about 7,000,000. Fig. 5 compares the velocity profiles under the air curtain supply inlet for different meshing strategies under a specific condition. The difference of the average velocity was within 7%. For the exfiltration flow rate, the difference was around 7% (7.5 kg/s for the strategy 1 and 7 kg/s for the strategy 2). The results of two different meshing strategies were reasonably close, so the meshing strategy 1 was selected (with the total grid number of about 1,260,000).

It is noted that for the simulation cases with a person model, the person model is simplified as a group of blocks, and is not a part of the fluid calculation domain. Since the person model is structured by cuboids

(Fig. 2), the whole fluid zone can still be meshed with structured hexahedral grids. The heat transfer process about the person model was also neglected.

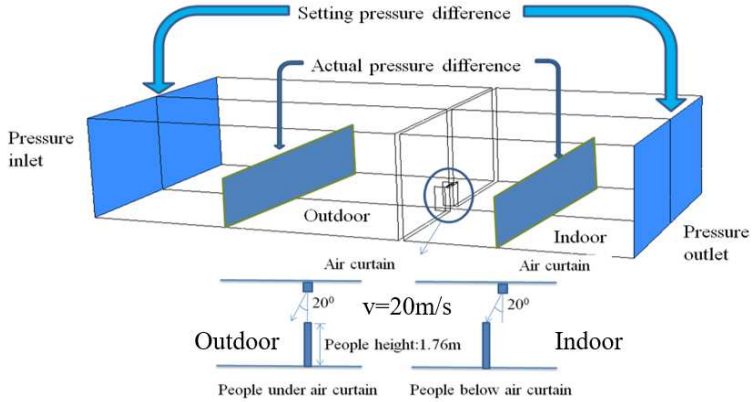

Fig. 4. CFD model of a full-size building and the location of people.

Using the CFD model (illustrated in Fig. 4), 708 CFD simulations were conducted for the air curtain door with the air curtain supplying air at 10, 15 and 20 m/s and 0°, 10°, 15° and 20° towards the outside. Table 2 presents a summary of all the simulation cases.

Table 2. CFD simulation cases with different supply speeds and angles.

	Winter mode	**Summer mode**
Outdoor temperature (℃)	-40, - 20, 10	25, 30, 40
Indoor temperature (℃)	21	24
Pressure difference (Pa)	-20, -10, -5, -3.5, -2.5, -1.5, -1, -0.5, 0, 10, 20, 30, 40	
Door opening angle (°)	90	
Air curtain supply speed (m/s)	10,15,20	
Air supply angle (°)	0*,10,15,20	
People location**	People below and under air curtain	
Total number of simulations	708 (438 cases without people, 270 with people)	

*0° air supply angle is only for cases with air supply speed of 15m/s

**Cases with people are under the condition of air supply velocity 20m/s and supply angle 20°

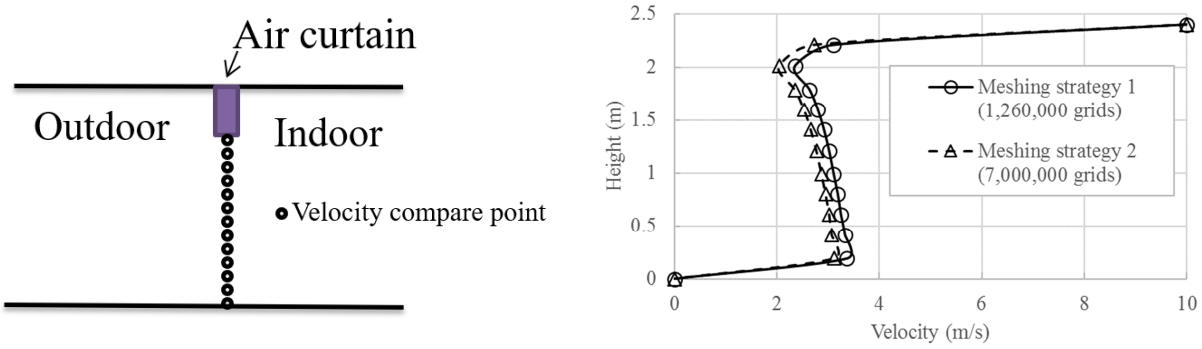

(a) Location of velocity comparing point. (b) Velocity comparison for different meshing strategies.

Fig. 5. Grid independent study (summer mode, outdoor temperature 25 °C, pressure difference -10 Pa, air curtain supply speed 10 m/s, supply angle 20°, without human model).

2.3. Infiltration model for door with air curtain

As suggested by Wang and Zhong [21], three flow patterns, optimum condition (OC), inflow break-through (IB) and outflow break-throught (OB), were observed and are shown in Fig. 6, and the corresponding Q- ΔP_{oi} relationship can be observed in Fig. 7. The optimum condition (Fig. 6a) is caused by mild outdoor and indoor pressure difference, ΔP_{oi}, and the jet is able to reach the floor and successfully blocks the outdoor air. In this case, there is still a net outflow portion as a result of the air curtain jet passing through the door. As ΔP_{oi} rises above a threshold value, which is defined as the upper critical pressure difference, ΔP_{uc}, the outdoor air would penetrate the jet as Fig. 6b shows. In this condition, the increase of pressure difference will result in increased infiltration. As the opposite flow pattern, Fig. 6c shows an outflow break-through when indoor pressure is higher than the outdoor pressure ($\Delta P_{oi} < 0$) and ΔP_{oi} reaches another threshold value, which is defined as the lower critical pressure difference, ΔP_{lc}, so the exfiltration of indoor air occurs.

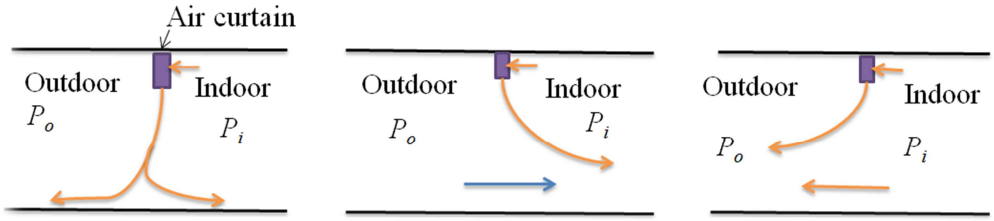

(a) Optimum condition (OC) (b) Inflow break-through (IC) (c) Outflow break-through (OB)

$\Delta P_{uc} < \Delta P_{oi} < \Delta P_{lc}$ $\Delta P_{oi} > \Delta P_{uc}$ $\Delta P_{oi} < \Delta P_{lc}$

Fig. 6. Characteristics of an air curtain jet under different pressure differences, $\Delta P_{oi}=P_o-P_i$ (adapted from [21]).

Previous studies have found that when air curtain is installed above the door, the infiltration flow rate is not only influenced by the features of the door opening area, but also the aerodynamics of the air curtain jet [21], and the orifice equation is not applicable [20,21,32]. For example, under the optimum condition in Fig. 6(a), the net airflow is not zero even if the pressure difference across an air curtain is zero. Therefore, the infiltration model of Eq. (1) for each of the above three scenarios is proposed, where an extra term is added to the orifice equation: the discharge modifier, D_D ($Pa^{0.5}$). Q is the net flow rate through the door opening, m^3/s. The discharge coefficients, C_D, and the discharge modifiers, D_D, can be correlated using Eq. (1) by the net flow rates, Q, and pressure differences, ΔP_{oi}, for each flow pattern, which can be obtained from experimental or numerical simulation results.

$$\frac{Q}{A\sqrt{2/\rho}} = sign(\Delta P_{oi}) C_D \sqrt{|\Delta P_{oi}|} + D_D \quad (1)$$

Where Q is flow rate in m^3/s, A is door opening area in m^2, ρ is air density in kg/m^3, and ΔP is the pressure difference across the door in Pa.

The upper critical pressures, ΔP_{uc}, and lower critical pressures, ΔP_{lc}, could be determined as shown in Fig. 7, which could be used to evaluate the performance of air curtain. A larger value of ΔP_{uc} indicates a better performance of the air curtain to block the air infiltration through the door opening. A larger pressure difference between ΔP_{uc} and ΔP_{lc} means a wider range of the optimum condition and therefore better air curtain performance. Therefore, the values of ΔP_{uc} and ΔP_{lc} are used to evaluate the performance of air curtain for the parametric study in this paper.

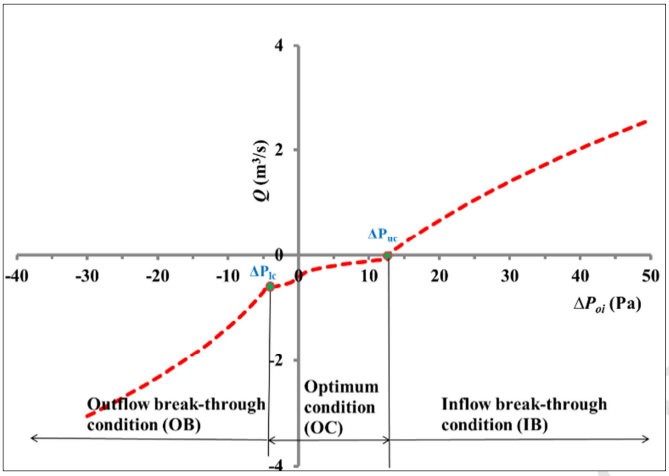

Fig. 7. Illustration of air curtain performance by using the Q-ΔP_{oi} relationship.

3. Results and discussions

3.1. Verification of CFD modeling approach

To validate the air curtain modeling method in CFD, the airflow through the CUBE chamber with air curtain was simulated under the condition of air supply speed of 9.1 m/s and 13.75 m/s and supply angle of 20° towards outside. The details of the CFD simulation setups can be found from our previous work [22]. The simulation results were compared with the experimental results and presented in Fig. 8. The comparison shows a good agreement between the experimental measurements and CFD simulations. Note that each CFD data point in Fig. 8 is one specific CFD simulation so we did not connect all the CFD data by lines.

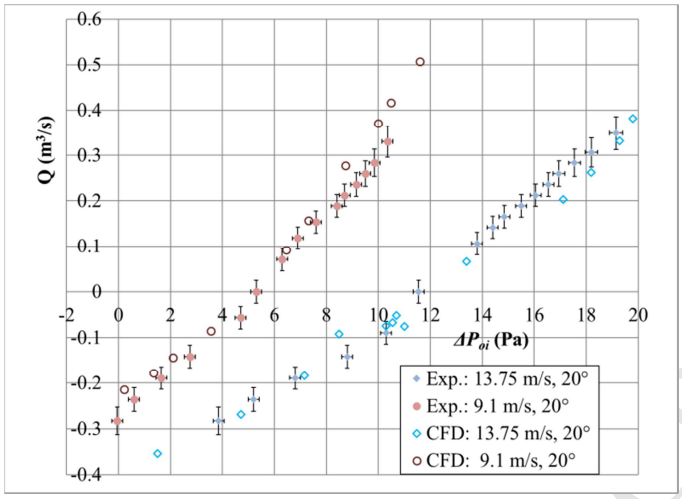

Fig. 8. Comparison of experiments and CFD simulations for the air curtains with different air speeds.

3.2. Parametric study - effect of air supply angle

Figure 9 presents the experimental results of the supply angle of 0° and 20° and for the supply speed of 9.1 m/s and 13.75 m/s. The air infiltration decreases significantly when the air supply angle increases from 0° to 20°. ΔP_{uc} increases from 5.5 Pa to 11.5 Pa when the supply angle increases from 0° to 20° for 13.75 m/s, and increases from 2.2 Pa to 5.5 Pa when the supply angle increases from 0° to 20° for 9.1 m/s. Thus, better air curtain performance could be achieved by increasing the supply angle when it is operated under the optimum and inflow break-through conditions.

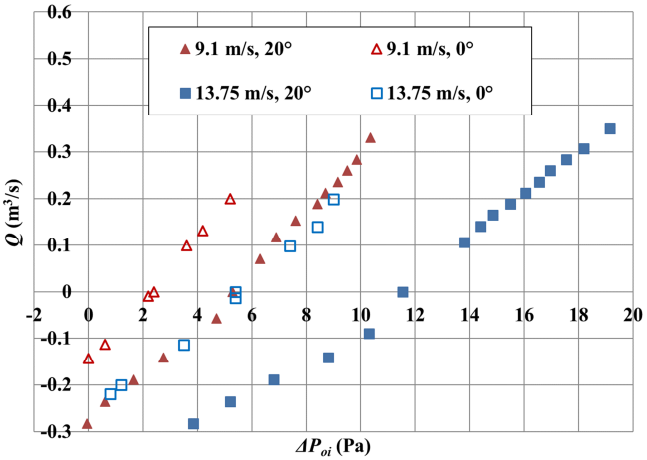

Fig. 9. Experimental results of the reduced-scale chamber with supply angle of 0° and 20° for both 9.1 m/s and 13.75 m/s.

Figure 10 shows the study of the supply angles on the air curtain performance based on the full-size CFD simulations. It can be seen that as the supply angle increases, there is slightly less infiltration but more exfiltration. Moreover, the higher the supply speed is, more effects of different supply angles are observed during in the OB regions. For example, there is no obvious difference of air exfiltration among different supply angles during the OB condition when the supply speed is 10 m/s (Fig. 10a). However, when the supply velocity is increased 20 m/s (Fig. 10b), exfiltration rate increases significantly as the supply angle increases, e.g., from 12 m^3/s to 15.5 m^3/s, when the supply changes from 10° to 20° for the case of 20 m/s at -20 Pa. The curves for the supply velocity of 15 m/s are similar to those of 20 m/s so they are not shown here.

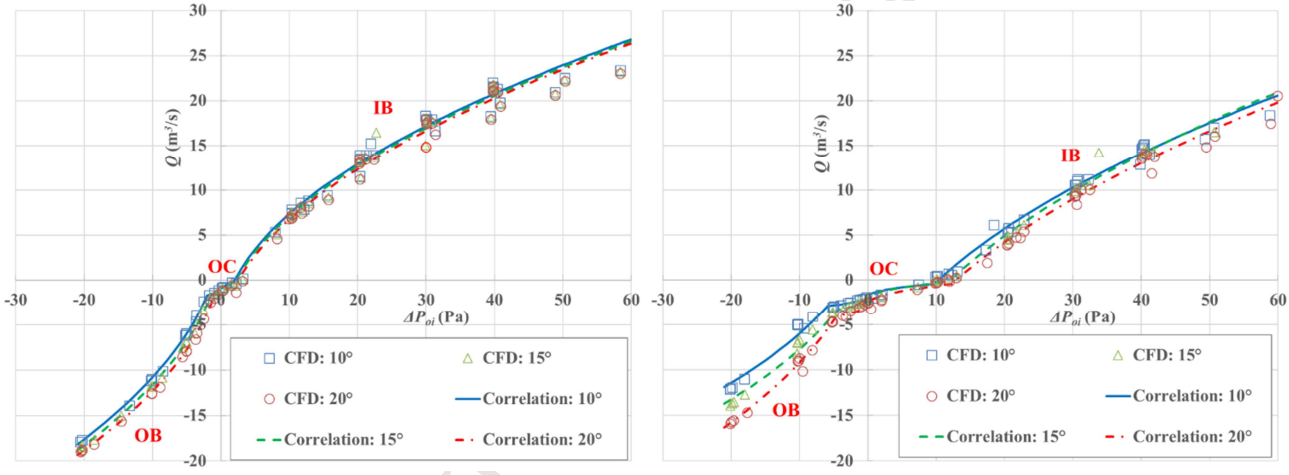

(a) (b)

Fig. 10. Results of the full-size CFD simulations for different air supply angles at the supply speed of (a) 10 m/s and (b) 20 m/s.

Figure 10 contains many data lines, which makes it hard to show a clear picture of the effect of supply angle. To provide a better insight, Figure 11 explains the influence of supply angle on the upper and lower critical pressure differences. It is apparent that as the supply angle increases, both ΔP_{uc} and ΔP_{lc} increase, indicating a larger supply angle is benificial for the air curtain's resisting effect against infiltration for the IB and OC conditions. The practical implication of this conclusion is that for an air curtain operating during the IB (e.g. a building is under-pressurized) or OC modes, it will be beneficial to point the air curtain supply vanes more outwards. On the other hand, the increase of ΔP_{lc} means an

earlier transition from the OC region to the OB, indicating exfiltration occurs earlier even at low pressure differences. Therefore, for an air curtain operating in the OB mode (for example, a building is over-pressurized), larger air curtain supply angle creates more infiltration at low pressure regions, which should be avoided. For example, when the supply velocity is 20 m/s, as the supply angle increase from 10° to 20°, the corresponding ΔP_{uc} increases from 10.3 Pa to 12.9 Pa, indicating the air curtain is able to resist a higher incoming pressure. This is consistent with the observations from Fig. 10. Therefore, it is very important to monitor the indoor and outdoor pressures so we will know at which mode the air curtain operates on the performance curve, and then choose to either increase or decrease the supply angle in order to reduce both infiltration and exfiltration through a doorway.

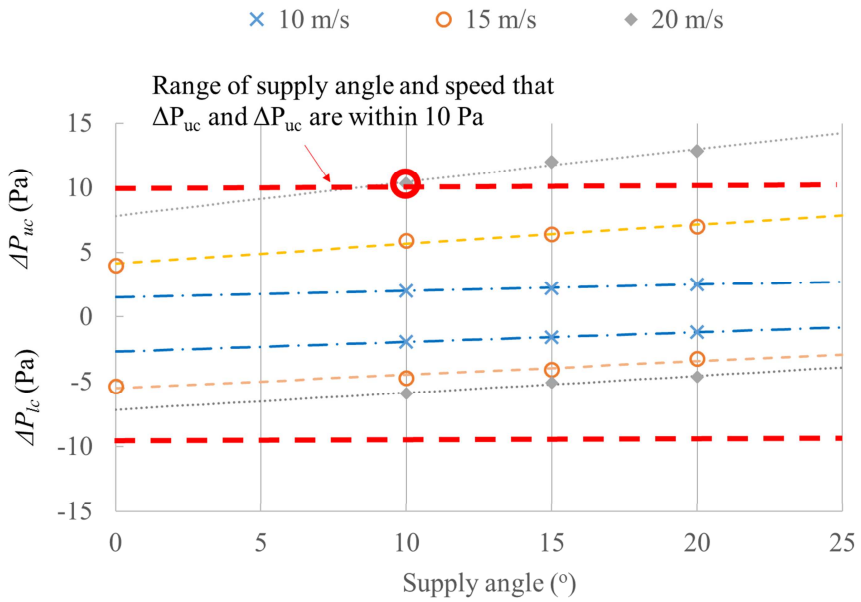

Fig. 11. Influence of supply angle on upper and lower critical pressure differences.

To minimize both infiltration and exfiltration, an air curtain should be operated to ensure that the monitored pressure difference across entrance door to fall within ΔP_{lc} or ΔP_{uc}. Suppose the annual pressure difference across the envelope for a typical building is within 10 Pa [35], Fig. 11 shows that the air curtain with the maximum air supply velocity of 20 m/s and the minimum supply angle of 10° will maintain the unit at the OC mode, i.e. $\Delta P_{uc} \approx 10$ Pa so that it is capable to reduce the infiltration/exfiltration significantly. This information provides key insights into air curtain operations and designs.

3.3. Parametric study - effect of air supply speed

Figure 12 plots the Q-ΔP_{oi} relationship for different air supply speeds at different supply angles. It shows that higher supply speed can significantly reduce the infiltration through the door, and increases the upper critical pressure, ΔP_{uc}, during the IB condition, when compared to lower speeds: the curve shift to the right with the increase of supply velocity. It is also important to note that for the same air curtain supply angle, higher supply speed also results in lower exfiltration, during OB condition. However, this effect becomes less significant when the supply angle becomes 20° (Fig. 12b) when compared to 10° (Fig. 12a): indicating that a larger supply angle towards outside will reduce the air curtain performance when indoor pressure is higher than outside.

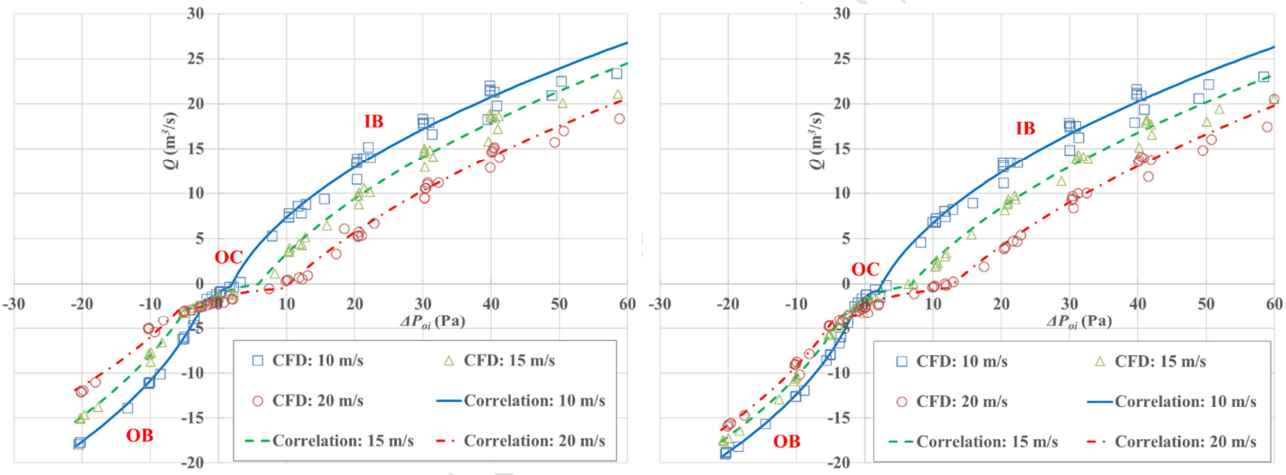

(a) (b)

Fig. 12. Results of the full-size CFD simulations for different air supply speeds at the supply angle of (a) 10° and (b) 20°.

3.4. Parametric study - effect of people in doorway

Figure 13 presents the experimental results obtained with the person model below the air curtain and those without the person. The comparative figure shows that the air curtain door performance seems unaffected by the person in presence. The PIV test results in Fig. 14 further prove this observation. Under the same pressure difference (ΔP_{oi} = 11.2 Pa), the captured PIV flow patterns at the door mid-plane show that the air curtain's jet moves around the person while still providing the appropriate sealing for the door against air infiltration with and without the person. It is important to note that some

of the measured disturbances observed in the PIV results are due to the existence of the person in the doorway which blocked the laser sheets behind the model (i.e. inside the chamber). Another reason is that the flow in the chamber and from the air curtain exhibited 3D flow characteristics and the PIV system only captured the 2D time-averaged flow at the middle plan.

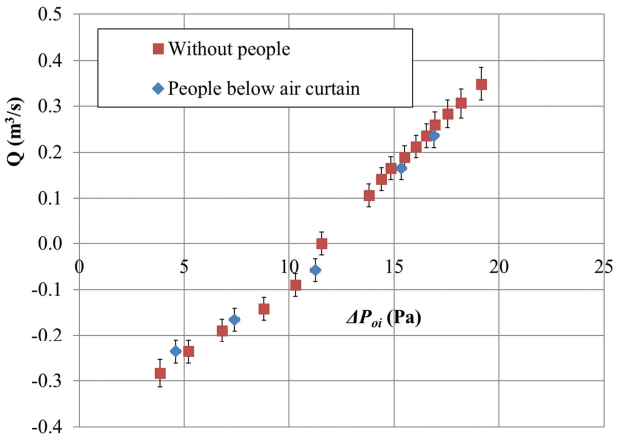

Fig. 13. Experimental results of the reduced-scale chamber with people below the air curtain jet of 13.75 m/s at the angle of 20°.

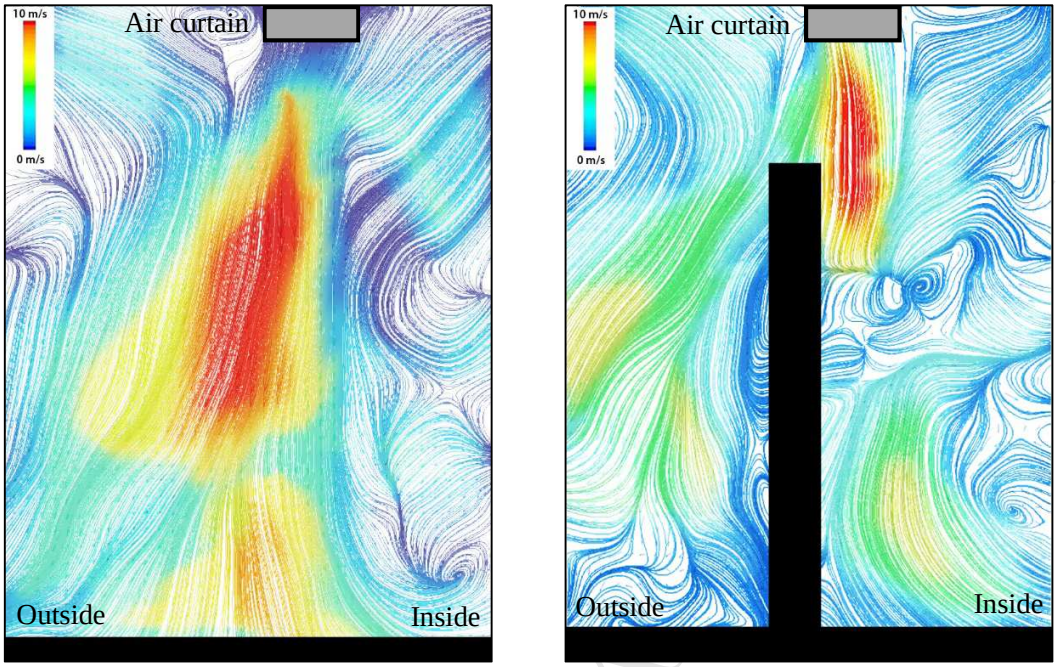

(a) Without people. (b) People below air curtain.

Fig. 14. PIV streamline measurements at the door mid-plane with air supply velocity: 13.75 m/s and angle: 20° for (a) without people, (b) dummy people below air curtain's jet (ΔP_{oi} = 11.2 Pa).

Fig. 15 shows the CFD velocity profile at the central section of the door when one person is below the air curtain. The results indicate that there still exist three flow patterns, inflow break-through, optimum condition and outflow break-through, though the air jet is affected by the person especially during the range of mild pressure difference (optimum condition). The same conclusions of the reduced-scale chamber tests also apply to the full-size CFD simulation results as shown in Fig. 16. With the person in the doorway, there still exist three distinct flow conditions. For the range of mild pressure difference (from -4 to 12.3 Pa), the existence of the person has little influence on the infiltration/exfiltration curve. With the increase of the pressure difference (in the IB region), a person in the doorway, either directly under or below the air curtain unit, contributes to more reduction of the infiltration due to the blockage from the person against the incoming air. This blockage effect is more apparent when the person is directly under the air curtain, i.e. the person standing right in the middle of the door), than when the person is below the unit. In summary, both experimental and numerical results show that the presence of

a person in the doorway, either directly under or below the air curtain, has little effect on air curtain performance, and in some scenarios, it even helps to block incoming air so the infiltration through the door is reduced.

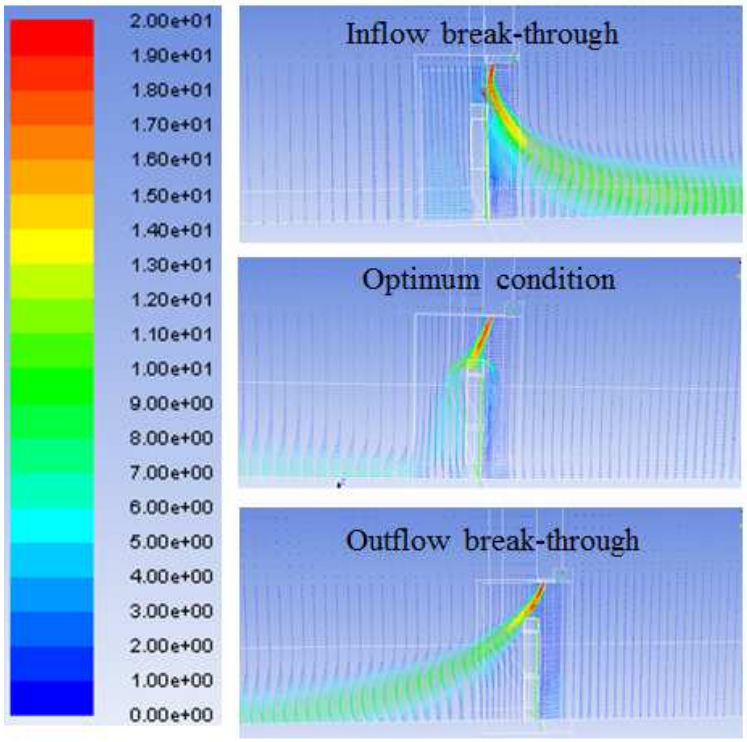

Fig. 15. CFD illustration of air flow pattern at the central section of the door (velocity, m/s).

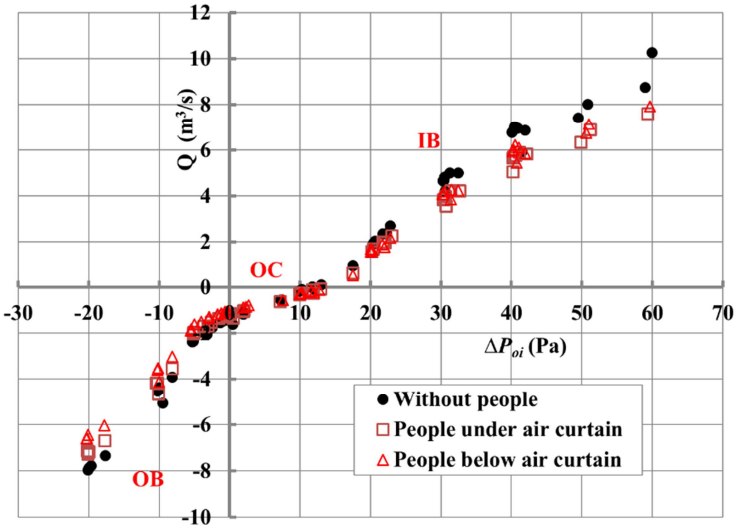

Fig. 16. Air curtain performance of the full-size CFD simulations with/without person in the doorway (supply angle: 20°).

It should be noted that the small-scale PIV tests here are used to exam air curtain flow patterns, rather than to validate full-scale CFD simulations. In fact, it is often impractical to validate full-size CFD results by full-size PIV tests because it is quite challenging to conduct full-size PIV experiments due to the space needed to project the laser light and the large size of the room [36]. Therefore, most of the previous PIV tests were conducted on small-scale experiments [37–39] or a section of a whole space [40–42]. Currently, validating full-scale CFD simulations by full-scale PIV experiments is fairly limited or non-exist in the most cases.

Mover, as mentioned in section 2.3, the focus of this paper is to study the effect of supply speed, angle and people on air curtain performance associated with the pressure difference parameters, i.e. the values of ΔP_{uc} and ΔP_{lc}, which are obtained from Q-ΔP_{oi} relationship (Fig. 7). Therefore, the CFD modeling approach is validated in the forms of Q-ΔP_{oi} relationship in section 3.1. The PIV test results were meant to providing extra information assisting the understanding of air curtain flow patterns so the PIV tests and using them for validating CFD models (in any case) are not the focuses of the current study. Validating CFD simulations of air curtains by PIV experiments has been one of the research focuses of our previous publication [22], which provides more information for readers with more interests in PIV tests and validation studies.

4. Conclusions

In this parametric study, 102 reduced-scale experiments and 708 full-size CFD numerical simulations were used to investigate the effect of the supply speed and angle as well as the effect of the presence of people on the performance of air curtain, and the infiltration/exfiltration rates through air curtain doors. Previous studies found that there exist three flow conditions (namely: optimum condition, inflow break-through and outflow break-through conditions) according to the characteristics of an air curtain jet under different pressure differences. During the optimum condition, the jet is able to reach the floor and successfully blocks the outdoor air, and therefore it is the objective condition for the design of air curtain. Considering the upper critical pressures, ΔP_{uc}, and lower critical pressures, ΔP_{lc}, are the key parameters to determine boundaries of the optimum condition, in this study they are used to evaluate the performance of air curtain with the designated various parameters. A larger value of ΔP_{uc} and more negative value of ΔP_{lc} indicate that a larger pressure difference across the door opening is required to generate infiltration break-through and exfiltration break-through condition, respectively. Thus, a larger value of ΔP_{uc} and more negative value of ΔP_{lc} are indicative of a better air curtain performance (or in

other words, a wider span of the optimum condition region). In this study, ΔP_{uc} and ΔP_{lc} are obtained by correlating the data of infiltration flow rates and the pressure differences across the door using the infiltration model for the door with air curtains. The experimental and numerical study found that:

(1) Increasing the supply angle will increase the values of ΔP_{uc} and ΔP_{lc}. Thus, the larger supply angle will improve the air curtain performance when it is operating under the optimum and infiltration break-through conditions. However, it will weaken the air curtain's performance of reducing exfiltration during outflow break-through condition.

(2) Increasing the supply speed of air curtain will increase the value of ΔP_{uc} and decrease the value of ΔP_{lc}. Thus, increasing the supply speed will contribute to lower infiltration/exfiltration during the infiltration break-through and exfiltration break-through conditions. Therefore, increasing supply speed could improve air curtain's performance. However, as the supply angle increases, the difference of the air curtain performance curve ($Q \sim \Delta P$) for different supply speed becomes smaller during the outflow break-through condition.

(3) Although the air curtain jet is affected by the person especially during the range of mild pressure difference (namely: optimum condition), it was found that the person has little influence on the infiltration/exfiltration during optimum condition (small pressure differences). However, since the person present in the doorway can contribute to the increase of the flow resistance through the door (i.e. to some extent improving the performance of the air curtain door), as the pressure difference across the door increases, the presence of the person can reduce the infiltration/exfiltration through the air curtain when compared to the cases without the person.

The findings of this study provide several key insights of air curtain and their performance contributors, which are important for designers, engineers, architects and building operators. There exist some other parameters, e.g. external wind speed and direction, and existence of indoor and outdoor temperature difference, which should be explored for the future study. Another step of the future study would be to employ the air curtain performance curves under different parameters from this study to conduct airflow and building energy analysis to evaluate their energy impacts from the perspective of the annual whole-building energy efficiency under different weather and air curtain operating conditions.

Acknowledgement

The authors acknowledge the financial and technical support from the Air Management and Control Association (AMCA), Mars Air Systems, Berner International, Powered Aire and InterCode Incorporated. The authors would also like to thank MËKANIC team for the construction of the experimental chamber as well as providing some of the professional images for the experimental setup used in this paper.

Reference

[1] B. Thornton, W. Wang, Y. Huang, M. Lane, B. Liu, Technical Support Document: 50% Energy Savings for Small Office Buildings, Pacific Northwest Natl. Lab. (2010).
[2] US DOE, 2011 Buildings Energy Data Book, 2012.
[3] S.J. Emmerich, A.K. Persily, Energy Impacts of Infiltration and Ventilation in U.S. Office Buildings Using Multizone Airflow Simulation, IAQ Energy 98. (1998) 191–203.
[4] S. Goubran, D. Qi, W.F. Saleh, L. Leon, Comparing methods of modeling air infiltration through building entrances and their impact on building energy simulations, Energy Build. 138 (2017) 579–590.
[5] ASHRAE, ASHRAE Handbook–Fundamentals, ASHRAE, Atlanta, 2013.
[6] K. Nicklas, Air Infiltration through Building Entrances, Chalmers University of Technology, 2013. http://publications.lib.chalmers.se/records/fulltext/184752/184752.pdf.
[7] G.K. Yuill, Impact of High Use Automatic Doors on Infiltration, ASHRAE Res. Proj. 763-TRP. (1996) 1–150.
[8] G.K. Yuill, R. Upham, H. Chen, Air leakage through automatic doors, ASHRAE Trans. 106 (2000) 145–160.
[9] ASHRAE 90.1, Energy standard for buildings except low-rise residential buildings, American Society of Heating, Refrigerating and Air-Conditioning Engineers Inc, Atlanta, GA, 2010.
[10] L. (Leon) Wang, Investigation of the Impact of Building Entrance Air Curtain on Whole Building Energy Use, Air Mov. Control Assoc. (2013) 1–57.
[11] S. Goubran, D. Qi, L. (Leon) Wang, Assessing dynamic efficiency of air curtain in reducing whole building annual energy usage, Build. Simul. 10 (2017) 497–507.
[12] J.J. Costa, L.A. Oliveira, M.C.G. Silva, Energy savings by aerodynamic sealing with a downward-blowing plane air curtain-A numerical approach, Energy Build. 38 (2006) 1182–1193.
[13] Y.G. Chen, Parametric evaluation of refrigerated air curtains for thermal insulation, Int. J. Therm. Sci. 48 (2009) 1988–1996.
[14] A.M. Foster, M.J. Swain, R. Barrett, P. D'Agaro, L.P. Ketteringham, S.J. James, Three-dimensional effects of an air curtain used to restrict cold room infiltration, Appl. Math. Model. 31 (2007) 1109–1123.
[15] T.C. Pappas, S.A. Tassou, Numerical investigations into the performance of doorway vertical air curtains in air-conditioned spaces, ASHRAE Trans. 109 PART 1 (2003) 273–279.
[16] Air Movement and Control Association International, Application Manual for Air Curtains, 2012.
[17] H. Giráldez, C.D. Segarra Pérez, I. Rodríguez, A. Oliva, Improved semi-analytical method for air

curtains prediction, Energy Build. 66 (2013) 258–266.
[18] J.C. Gonçalves, J.J. Costa, a. R. Figueiredo, a. M.G. Lopes, CFD modelling of aerodynamic sealing by vertical and horizontal air curtains, Energy Build. 52 (2012) 153–160.
[19] F.C. Hayes, Heat transfer characteristics of the air curtain: a plane jet subjected to transverse pressure and temperature gradients, University of Ilinois, 1968.
[20] F.C. Hayes, W.F. Stoecker, Design Data For Air Curtains, ASHRAE Trans. (1969) 168–180.
[21] L.L. Wang, Z. Zhong, An approach to determine infiltration characteristics of building entrance equipped with air curtains, Energy Build. 75 (2014) 312–320.
[22] S. Goubran, D. Qi, W.F.W.F. Saleh, L. Wang, R. Zmeureanu, Experimental study on the flow characteristics of air curtains at building entrances, Build. Environ. 105 (2016) 225–235.
[23] New Wave Research, Solo PIV - Nd : YAG Laser Systems, (2004).
[24] Laser Optical CCD and sCMOS Cameras | Dantec Dynamics, (n.d.).
[25] F. Scarano, S. Ghaemi, G. Caridi, J. Bosbach, U. Dierksheide, A. Sciacchitano, On the use of helium - filled soap bubbles for large - scale Tomographic PIV wind tunnel experiments, Exp. Fluids. 56 (2015) 7–10. doi:10.1007/s00348-015-1909-7.
[26] J. Bosbach, M. Kühn, C. Wagner, M. Raffel, C. Resagk, R. Puits, A. Thess, Large Scale Particle Image Velocimetry of Natural and Mixed Convection 2 . Measurement of Convective Air Flow on Large Scales, (2006) 26–29.
[27] A. Li, L. Gou, X. Wang, Y. Zhang, 2D-PIV experiment analysis on the airflow performance of a floor-based air distribution with a novel mushroom diffuser (FBAD-MD), Energy Build. 121 (2016) 114–129. doi:10.1016/j.enbuild.2016.03.075.
[28] X. Cao, J. Liu, N. Jiang, Q. Chen, Particle image velocimetry measurement of indoor airflow field: A review of the technologies and applications, Energy Build. 69 (2014) 367–380. doi:10.1016/j.enbuild.2013.11.012.
[29] ANSYS, ANSYS FLUENT User's Guide – Release 12.0, Canonsburg, PA, 2011.
[30] Z. Lian, D. Qi, L. Weiwei, Influence of indoor partition on air distribution of ceiling-mounted cassette type indoor unit, J. Cent. South Univ. 41 (2010) 363–369.
[31] American Association of Automatic Door Manufacturers (AAADM). Automatic Door Selection Guide, 2007. doi:http://www.aaadm.com/pdfs/Selection%20Guide-503.pdf.
[32] M. Shields, S. Gorber, M. Tremblay, Methodological issues in anthropometry: Self-reported versus measured height and weight, Proc. Stat. (2008) 1–10. http://www.statcan.gc.ca/pub/11-522-x/2008000/article/11002-eng.pdf.
[33] Q. Chen, Ventilation performance prediction for buildings: A method overview and recent applications, Build. Environ. 44 (2009) 848–858. http://dx.doi.org/10.1016/j.buildenv.2008.05.025.
[34] ANSYS FLUENT 14.0 user guide, 2011.
[35] E. ČSN, 13829 Thermal performance of buildings–Determination of air permeability of buildings–Fan pressurization method, ČNI, Praha, 2000.
[36] Q. Chen, K. Lee, S. Mazumdar, S. Poussou, L. Wang, M. Wang, Z. Zhang, Ventilation performance prediction for buildings: Model assessment, Build. Environ. 45 (2010) 295–303.
[37] P. Karava, T. Stathopoulos, A.K. Athienitis, Airflow assessment in cross-ventilated buildings with operable façade elements, Build. Environ. 46 (2011) 266–279.
[38] R. Ramponi, B. Blocken, CFD simulation of cross-ventilation for a generic isolated building: Impact of computational parameters, Build. Environ. 53 (2012) 34–48.
[39] C. Sanjuan, M.J. Suárez, E. Blanco, M.D.R. Heras, Development and experimental validation of a simulation model for open joint ventilated façades, Energy Build. 43 (2011) 3446–3456.

[40] G. Cao, M. Sivukari, J. Kurnitski, M. Ruponen, O. Seppänen, Particle Image Velocimetry (PIV) application in the measurement of indoor air distribution by an active chilled beam, Build. Environ. 45 (2010) 1932–1940.
[41] X. Cao, J. Li, J. Liu, W. Yang, 2D-PIV measurement of isothermal air jets from a multi-slot diffuser in aircraft cabin environment, Build. Environ. 99 (2016) 44–58.
[42] J. Li, J. Liu, C. Wang, M. Wesseling, D. Müller, PIV experimental study of the large-scale dynamic airflow structures in an aircraft cabin: Swing and oscillation, Build. Environ. 125 (2017) 180–191.

Highlights

- Air curtain speed, angle and person presence manifest different aerodynamics impacts for different flow regions
- Wider span of optimum flow region at higher pressure difference indicates better air curtain performance
- Larger supply speed widens optimum flow region thus reduces both door infiltration and exfiltration
- Larger outward angle reduces infiltration in optimum and inflow breakthrough regions but increases exfiltration
- Doorway person presence adds minimum impact on the jet but more resistance against infiltration/exfiltration